Fuel 328 (2022) 125270

Contents lists available at ScienceDirect

Fuel

journal homepage: www.elsevier.com/locate/fuel

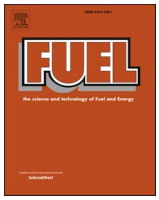

Full Length Article

Study on using graphene and graphite nanoparticles as fuel additives in waste cooking oil biodiesel

Vikas Sharma [a,b,c,1], Abul Kalam Hossain [a,b,c,1], Alamgir Ahmed [a,1], Ahmed Rezk [a,b,c,1,*]

[a] Department of Mechanical, Biomedical and Design Engineering, College of Engineering and Physical Science, Aston University, Birmingham B4 7ET, UK
[b] Energy and Bioproducts Research Institute (EBRI), College of Engineering and Physical Science, Aston University, Birmingham B4 7ET, UK
[c] Aston Institute of Materials Research (AIMR), College of Engineering and Physical Science, Aston University, Birmingham B4 7ET, UK

ARTICLE INFO

Keywords:
Biodiesel
Combustion
Emissions
Graphene
Graphite
Nanoparticle

ABSTRACT

Utilising waste cooking oil biodiesel in internal combustion engines for power generation and transport is of increasing importance, as it is the least pollutant disposal method for waste cooking oil. Besides, researchers have recently shown an increasing interest in utilising graphene and its derivatives in different applications due to its unique thermal and physical characteristics, including enhancing the combustion characteristics of biofuels. Therefore, this article studies the characteristics of waste cooking oil biodiesel blended with few-layered graphene and graphite nanoparticles additives and their influence on combustion and engine emissions and benchmark them against neat biodiesel and diesel fuels. The biodiesel was synthesised through a transesterification method from waste cooking oil and blended with diesel or butanol after adding few-layered graphene and graphite nanoparticles. Few-layered graphene and graphite nanoparticle additives led to greater peak in-cylinder pressure by 0.5–2.5% increment and 1–4% lower heat released rate at full load. As such, employing few-layered graphene and graphite in a fuel mix reduced NOx emission by 0.7–5 % compared to 100% diesel counterpart. Besides, at full engine load, waste cooking biodiesel blended with 100 ppm few-layered graphene and graphite nanoparticles showed an increment in brake thermal efficiency by 8–10% compared to pure fossil diesel and waste cooking biodiesel. The results show the feasibility of using graphene-based nanoparticle additives in biodiesel to enhance biodiesel fuel combustion characteristics, hence lowering NOx emissions.

1. Introduction

Worldwide energy consumption is continuously growing. It is no longer viable to rely on fossil-based energy sources such as petroleum, natural gas, and coal because of their finite availability and negative environmental impacts [1,2]. In addition, fossil-based energy sources are highly pollutant and cause carbon intensified emissions that cause global warming and ozone depletion. Therefore, there has been an increasing demand for renewable-based alternative sources for real-life applications [1,2]. Among the available renewable-based energy sources, biomass is the most resilient and has impacts far more minor than fossil fuels. Moreover, it is the most widespread, as it accounts for 80% of the renewable-based energy generated worldwide, specifically for transportation, heating, and power generation [1,2].

Recently, there has been an increasing interest in utilising waste cooking oil (WCO) to produce alternative fuels for Compression Ignition (CI) engines, as it is considered the least pollutant disposal method of WCO and to foster the diversity of energy mix and circular bioeconomy [3,4]. To virtually combust WCO in IC engines, it could be mixed with petroleum diesel, preheated, or undergoes a transesterification process to produce biodiesel [5–7]. The critical merits of WCO-based biodiesel are its affordability, inborn lubricity, and suitability for CI with minimal fundamental modifications to the engine design or structure [8,9]. Moreover, CI engines are widely used for power generation and transportation. Therefore, utilising WCO-based biodiesel in such applications can promote the uptake of bioenergy to foster the circular economy in many Societies. On reflection, Khan et al. [10] investigated the viability of using WCO-based biodiesel in Pakistan and developed a decision-making metric to alleviate the national economic burdens due to the substantial fossil fuel imports.

There are several benefits of utilising biofuels, including WCO-based

* Corresponding author at: Department of Mechanical, Biomedical and Design Engineering, College of Engineering and Physical Science, Aston University, Birmingham B4 7ET, UK.
E-mail address: a.rezk@aston.ac.uk (A. Rezk).
[1] The authors contributed equally

https://doi.org/10.1016/j.fuel.2022.125270
Received 26 March 2022; Received in revised form 19 June 2022; Accepted 8 July 2022
Available online 14 July 2022

Nomenclature

%	Percentage
°C	Degree Celsius
°CA	Degree crank angle
aTDC	After top dead centre
bTDC	Before top dead centre
BTE	Brake Thermal Efficiency
BD	Burn duration
BSFC	Brake specific fuel consumption
B40	40% WCB, 40% Fossil Diesel and 20% Butanol
B40NCP0.5	40% WCB, 40% Fossil Diesel and 20% Butanol with 50 ppm of Graphene
B40NCP1	40% WCB, 40% Fossil Diesel and 20% Butanol with 100 ppm of Graphene
B40C0.5	40% WCB, 40% Fossil Diesel and 20% Butanol with 50 ppm Graphite
B40C1	40% WCB, 40% Fossil Diesel and 20% Butanol with 100 ppm Graphite
B50	50% Waste Cooking Biodiesel, 40% Fossil Diesel and 10% Butanol
B50NCP0.5	50% WCB, 40% Fossil Diesel and 10% Butanol with 50 ppm Graphene
B50NCP1	50% WCB, 40% Fossil Diesel and 10% Butanol with 100 ppm Graphene
B50C0.5	50% WCB, 40% Fossil Diesel and 10% Butanol with 50 ppm Graphite
B50C1	50% WCB, 40% Fossil Diesel and 10% Butanol with 100 ppm Graphite
B80	80% WCB and 20% Butanol
B80NCP0.5	80% WCB and 20% Butanol with 50 ppm Graphene
B80NCP1	80% WCB and 20% Butanol with 100 ppm Graphene
B80C0.5	80% WCB and 20% Butanol with 50 ppm Graphite
B80C1	80% WCB and 20% Butanol with 100 ppm Graphite
B90	90% WCB and 10% Butanol
B90NCP0.5	90% WCB and 10% Butanol with 50 ppm Graphene
B90NCP1	90% WCB and 10% Butanol with 100 ppm Graphene
B90C0.5	90% WCB and 10% Butanol with 50 ppm Graphite
B90C1	90% WCB and 10% Butanol with 100 ppm Graphite
CV	Calorific value
CI	Compression Ignition
CA	Crank angle
CO	Carbon monoxide
CO2	Carbon dioxide
C	Graphite
D100	100% Fossil Diesel
EoC	End of combustion
FP	Flash point
HRR	Heat release rate
HRRmax	Maximum heat release rate
ID	Ignition delay
IP	Injection pressure
IHRR	integrated heat release rate
IDI	indirect injection
NP	nanoparticles
NO	nitric oxide
NCP	Graphene layers
Pmax	Maximum pressure
ppm	Parts per million
SoC	start of combustion (SoC),
TDC	Top dad centre
WCOB	waste cooking oil (WCO)

biodiesel. The oxygen content in biodiesel is generally about 10% compared to non in petroleum diesel. On the one hand, it reduces exhaust gas emissions such as hydrocarbon, PM, CO_2, and CO but could slightly increase NOx [11,12]. On the other hand, the low heating value and cetane number of WCO-based biodiesel, 8–10% lower than petroleum diesel, slightly reduces the maximum engine torque and increases brake specific fuel consumption (BSFC) [11,12]. Using biofuel blends (e.g., biodiesel-ethanol) is an avenue to enhance its combustion properties, enhance the NOx emission presence, and overcome other physiochemical drawbacks such as poor solubility in cold climates [13]. Alternatively, biodiesel's NOx emission and specific fuel consumption can be enhanced using oxygenated additives such as triethylene glycol mono-methyl-ether [14]. Furthermore, controlling the combustion emissions alleviates the need for after-treatment equipment that affects the CI engine's overall performance, such as increasing pumping power [15].

Using nanoparticles (NPs) additives in biofuel is an emerging approach to enhance the combustion of biofuels and boost engine performance [15,16]. The advanced thermal characteristics combined with the exceptionally high surface area per unit volume of nanoparticle additives provide a wide dynamic surface for chemical reactions. Based on a review study by Bidir et al. [16], over a wide range of nanoparticle additives, an enhancement of BSFC by up to 23%, brake power by up to 2.5%, and a significant reduction in CO and PM emission were concluded. Ferrão et al. [17] investigated the combustion characteristics of hydro-processed vegetable oil blended with aluminium nanoparticles at different sizes (40 nm and 70 nm) and concentrations (0.5 wt% and 1.0 wt%). The combustion rate of the biofuel was enhanced by increasing the nanoparticle concentration simultaneously with reducing the particle size by up to 42.5% at 40 nm and 1.0 wt% combination.

Using oxygenated nanoparticles could also enhance the emissions of biofuel combustion. Ağbulut et al. [18] studied the use of aluminium oxide (Al_2O_3) and titanium oxide (TiO_2) nanoparticles at 100 ppm concentration in diesel-bioethanol fuel blends and benchmarked them against conventional diesel fuel and diesel-bioethanol blend without nonadditive. The wider surface area per unit volume of Al_2O_3 and TiO_2 nanoparticles additives, their advanced thermophysical properties, and the oxygen contents enhanced the combustibility of diesel-bioethanol (DF90E10) fuel blends. They reported that compared to neat diesel, the NOx gas emission without nano-additive was increased by 3.6%. On the other hand, the NOx emission was decreased by 3.02% and 1.57%, respectively, when Al_2O_3 and TiO_2 nanoparticles additives were added separately in DF90E10 blends [18]. Purushothaman et al. [19] investigated the optimal quantity of Al_2O_3 and TiO_2 nanoparticles using mahua oil-based biodiesel. Jaikumar et al. [20] did other work on using oxygenated nanoparticles, Chromium oxide (Cr_3O_3), in Flaxseed oil biodiesel, which enhanced the engine performance and the emission level of the tested diesel engine.

Many researchers investigated nanoparticle additives in WCO-based biodiesel. Jabraeili et al. [21] investigated the utilisation of Al_2O_3-SiO_2 nanocomposite blended with WCO-based biodiesel at different concentrations (30, 60, 90, and 100), which enhanced the brake power and torque by up to 1.44% and 1.64%, respectively, compared to petroleum diesel fuel. Using Zinc oxide (ZnO) nanoparticle additives to WCO-based biodiesel, Lobo et al. [22] enhanced the BSFC, HC, CO, and NOx. Employing the exhaust gas recirculation (EGR) boosted the reduction of NOx from 15% to 20%; however, the low calorific value of the blend negatively affected the peak pressure value hence the BP and BTE. Cerium oxide nanoparticles were added to WCO-based biodiesel at different concentrations and combusted in variable compression ratio diesel engine, which enhanced the BTE and BSFC by 3.62% and 3.3%, respectively, compared to petroleum diesel addition to a considerable

enhancement in CO and NO_x emission.

Graphene is a single layer of carbon atoms arranged in a hexagonal shape. A single graphene layer exhibits a high thermal conductivity of up to 5300 W/mK and a high surface area of about 2600 m^2/g [23]. However, the thermal conductivity of graphene-based materials can be reduced by increasing the number of carbon atomic layers [24]. For example, graphite consists of stacked graphene layers of 1950 W/mK bulk thermal conductivity. The advanced thermal characteristics of graphene and its derivatives drew scientists' attention to enhancing biofuels' combustion characteristics. Therefore, Hoseini et al. [25] investigated the effect of graphene oxide (GO) additive on Ailanthus altissima biodiesel blends. Given the advanced thermal characteristics of GO and oxygen contents, it enhanced the brake power, SFC, and CO & HC emissions but increased NOx because of increasing the combustion temperature. In 2020, GO additives into biodiesel were produced from a wide range of feedstocks, such as Oenothera Lamarckian, Ailanthus altissima, Camelina sativa, and rice bran oil, were investigated. Similar trends in engine performance and emissions were observed [26–28]. In 2021, Ettefaghi et al. [29] investigated the use of graphene quantum dots as biodegradable nanoparticles additive to a diesel–biodiesel-water blend. The developed blend enhanced the brake power, SFC, and HC and reduced NOx by 3.8%. Chacko et al. [30] investigated GO and Graphene nanoplatelets (GNP) additives into WCO-based biodiesel and benchmarked it against petroleum diesel and Karanja-based biodiesel. GNP outperformed GO additives in NO, CO, and HC emissions, which concluded that GO and GNP are promising fuel additives for better emission control without significant effects on engine parts such as injector wear.

Given the current literature, the most recent research works emphasise using GO, NGP, and other metal nanoparticle additives for various biofuels. However, the effect of a broader range of low-cost graphene-based additives, such as graphite nanoparticles, is yet to be understood. Therefore, this work aims to study the broader application of few-layered graphene and graphite as fuel additives to enhance the engine's emissions combustion characteristics. Accordingly, three key objectives were identified: **(1)** developing four base blends of waste cooking oil biodiesel, diesel and 1-butanol such as B40 (40% Waste Cooking Biodiesel, 40% Fossil Diesel and 20% Butanol), B50 (50% Waste Cooking Biodiesel, 40% Fossil Diesel and 10% Butanol), B80 (80% Waste Cooking Biodiesel and 20% Butanol) and B90 (90% Waste Cooking Biodiesel and 10% Butanol) respectively; **(2)** developing multi-component fuel blends by adding few-layered graphene (NCP) and graphite (C) at 50 ppm and 100 ppm; **(3)** studying the combustion and engine emission characteristics for selected three of 20 developed blends: B40, B40NCP1 (40% Waste Cooking Biodiesel, 40% Fossil Diesel and 20% Butanol with 100 ppm of graphene) and B40C1 (40% Waste Cooking Biodiesel, 40% Fossil Diesel and 20% Butanol with 100 ppm graphite).

2. Materials and methods

Waste cooking oil (WCO) was selected to synthesise the biodiesel blend due to its widespread availability, the increasing interest in using it in CI engines as the least pollutant disposal method and, foster the circular bioeconomy. Used sunflower cooking oil was obtained from the University food court. Potassium hydroxide (KOH), butanol (98% purity), and methanol (98% purity) were sourced from Thermo Fisher Scientific. Few-layered graphene (1–5 carbon layers) was sourced from Graphitene ltd. Graphite nanoparticles were sourced from Sigma Aldrich. Butanol was procured from Fisher Scientific Ltd.(UK).

2.1. Biodiesel synthesis

Transesterification, a well-known chemical technique, was used to synthase WCO-biodiesel (WCOB) in batches of 2 L each. First, 1 L of raw WCO was placed into a round bottom flask and heated to 55 °C second, a methylic solution consisting of methanol and KOH was added to the warmed oil and agitated at 600 rpm for 1 h. The methylic solution constituted a 4:1 methanol-to-oil ratio and 1 wt% KOH of the oil weight. The mixture was then transferred to a separating funnel to settle overnight. As a result, a black glycerol layer was formed at the bottom and a light methyl ester layer (ME) formed on the top. The glycerol was removed, and the biodiesel was washed with distilled water at 90 °C to remove any remaining methanol. After one hour, the washed fuel was heated at 105 °C to remove moisture content, and a dry WCOB was obtained.

2.2. Nanoparticle blends synthesis

In this study, butanol was used to dilute the nano-emulsified fuel. Butanol has distinct properties that help prepare stable fuel blends and act as a fuel binder [31,32]. Literature suggested that up to 20% butanol can be used in the fuel blends to achieve optimum engine performance and combustion characteristics [31,32]. Firstly, four base samples were prepared by blending WCOB, diesel and butanol: B40, B50, B80, and B90, as shown in Table 2. Secondly, NCP and C were added at 50 ppm and 100 ppm. The nanoparticles are depicted in Fig. 1, and their properties are furnished in Table 1. 20 blends were prepared from graphene and graphite NP, as given in Table 2. A two-step mixing process was achieved to develop a homogeneous dispersion: a magmatic stirrer for 15 min followed by an ultrasonic bathtub at 50 kHz for 30 min, as shown in Fig. 2. The developed nanoparticle blends are shown in Fig. 3.

2.3. Engine experimental setup

The combustion characterisation experiments were conducted on a naturally aspirated Lister Petter Alpha series, water-cooled, three-cylinder indirect injection (IDI) diesel engine, as sketched in Fig. 4. The engine's parameters are listed in Table 3. The engine was controlled to maintain its speed at 1500 rpm while the torque varied. Five engine loads were used for this study: 20 % (1.9 kW), 40 % (3.8 kW), 60 % (5.7 kW), 80 % (7.6 kW), and 100 % (9.75 kW). A Froude Hofman AG80HS eddy current dynameter was used to load the engine. A Kistler pressure sensor (Kistler 6125C11) was installed in the cylinder head to record the in-cylinder pressure, and a crank angle encoder (model) was placed on the crankshaft record the crank angle position. A fuel pressure sensor (model - Kistler 4618A0 sensor) was attached to the fuel line near the head of the fuel injector. All three sensors were integrated with a data logger KiBox supplied by the Kistler Instruments Ltd. KiBox software was used to analyse the combustion data by taking an average of 51 cycles and generated in-cylinder pressure, heat release, and fuel injection pressure concerning crank angle Bosch BEA 850 gas analyser was used to test engine exhaust gas emissions. The instrument's specifications are provided in Table 4.

3. Results and discussions

3.1. Fuel characteristics

The instruments used for the measurement of various physical and chemical properties are Canon Fenski u-tube viscometers (with a measurement uncertainty of between 0.16% and 0.22%) and a thermostatic water bath (±0.1° C) to measure the kinematic viscosities; densities were measured using a hydrometer according to ASTM-D7544; Parr 6100 bomb calorimeter was used to measure the higher heating values (HHV). The flash point was measured using a Setaflash series 3 plus closed cup flash point tester (model 33000–0) according to ASTM121 D1655 standard. The measurement accuracies of the calorimeter and the flash point tester were ± 0.1% and ± 0.5. Properties of butanol were taken from literature and shown in Table 5.

The blends' properties were measured and compared to fossil diesel and W100 (Fig. 5), including heating value, viscosity, and flash point

Fig. 1. Pictorial view of the nanoparticles additives.

Table 1
Specification of nanomaterials.

Characteristics	Graphite	Graphene
Carbon content (%)	>95	>95
Bulk density (g/cm^3)	0.85	0.33
Flake thickness (layer)	1–5	> 10
Flake size (μm)	0.5–20	< 20
Thermal conductivity/(W/(m*K))	4.57	7.36
Thermal diffusivity/(mm^2/s)	4.92	22.23

Table 2
List of prepared blend fuel samples.

Sample No.	Fuel blends	Details
1	D100	100% Fossil Diesel
2	W100	100 % waste cooking oil biodiesel
3	B40	40% WCB, 40% Fossil Diesel and 20% Butanol
4	B40NCP0.5	40% WCB, 40% Fossil Diesel and 20% Butanol with 50 ppm of Graphene
5	B40NCP1	40% WCB, 40% Fossil Diesel and 20% Butanol with 100 ppm of Graphene
6	B40C0.5	40% WCB, 40% Fossil Diesel and 20% Butanol with 50 ppm Graphite
7	B40C1	40% WCB, 40% Fossil Diesel and 20% Butanol with 100 ppm Graphite
8	B50	50% Waste Cooking Biodiesel, 40% Fossil Diesel and 10% Butanol
9	B50NCP0.5	50% WCB, 40% Fossil Diesel and 10% Butanol with 50 ppm Graphene
10	B50NCP1	50% WCB, 40% Fossil Diesel and 10% Butanol with 100 ppm Graphene
11	B50C0.5	50% WCB, 40% Fossil Diesel and 10% Butanol with 50 ppm Graphite
12	B50C1	50% WCB, 40% Fossil Diesel and 10% Butanol with 100 ppm Graphite
13	B80	80% WCB and 20% Butanol
14	B80NCP0.5	80% WCB and 20% Butanol with 50 ppm Graphene
15	B80NCP1	80% WCB and 20% Butanol with 100 ppm Graphene
16	B80C0.5	80% WCB and 20% Butanol with 50 ppm Graphite
17	B80C1	80% WCB and 20% Butanol with 100 ppm Graphite
18	B90	90% WCB and 10% Butanol
19	B90NCP0.5	90% WCB and 10% Butanol with 50 ppm Graphene
20	B90NCP1	90% WCB and 10% Butanol with 100 ppm Graphene
21	B90C0.5	90% WCB and 10% Butanol with 50 ppm Graphite
22	B90C1	90% WCB and 10% Butanol with 100 ppm Graphite

temperatures. Table 5 and Fig. 5 show the properties of 22 tested samples, including five base fuel blends and NP-additive blends. The density test was conducted at room temperature (18 °C). W100 showed the highest density of 0.88 g/m^3, reducing the density when mixed with diesel and butanol. The density of B40, B40NCP1, B40NCP0.5, B40C1 and B40C0.5 were lower than W100 by 3.86 %, 3.7%, 3.8%, 3.9% and 3.97%, as shown in Fig. 5. Besides, the higher NCP and C additive percentages, the higher the blend's density, agreeing with Bidir et al. [16]. For example, B40NCP1 (0.847 g/m^3) density was higher than B40NCP0.5 (0.846 g/m^3). Blends with NCP additives showed an averagely of 1.5% higher density than fossil diesel fuel.

Biodiesel and other blends' viscosity were measured at 40 °C according to EU and ASTM standards.

The viscosity of W100 (5.563 cSt) was higher than the standard limits; therefore, it may be challenging to use neat biodiesel in the engine. The viscosity of the blend fuels was observed within the usable limits as this diluted by the addition of diesel and butanol. The addition of nanoparticles also influenced the viscosity of the fuel; it slightly increased. For example, the viscosity of B40NCP1 (3.262 cSt) was higher than B40 (2.864) (Table 5). The viscosity is not increasing for B50, B80 and B90 blends with the increase of nano-additive.

In contrast, it was observed that for blend B40, the viscosity was influenced by increasing the nanoparticle doses. Blend B40 consists of 40% W100 + 40%diesel + 20%biodiesel, the share of W100 is less in this blend. So, the B40 blend gave lower viscosity, close to fossil diesel fuel. In the case of B50, B80 and B90, the share of W100 was increased, which led to increasing the viscosity. These samples already have high viscosity; hence, when a small amount of nanoparticle was added, the viscosity of these blends was not noticeable.

Flash point (FP) is the lowest temperature at which the fuel vapour ignites, determining the safe storage condition. W100 showed the highest FP of 165 °C, as the flash point was reduced for all blends due to butanol addition. The FP for all the blends lies between diesel fuel and biodiesel fuel, within the biodiesel standards limits (Table 5). In addition, it was observed that changing the NCP and C additive percentage influenced the developed blends' flash point marginally. The percentage changes concerning diesel fuels are presented in Fig. 5. B80 blend gave lower FP than B50; the fluctuation in FP is mainly due to the addition of butanol. Butanol is highly volatile and has a lower flash point than diesel and biodiesel. While testing the FP of the blend samples, there is a possibility that butanol made combustible vapour with few amounts of biodiesel vapour and gave a lower flash point.

Diesel fuel showed the highest calorific value (CV) due to oxygen deficiency, as biofuel blends bound 9–11% oxygen [35]. In addition, butanol lowered the CV of the developed blends due to its lower CV and higher latent heat of vaporisation. The presence of fossil diesel in B40 and B50 blends led to CVs relatively higher than B80 and B90. The relatively high calorific values of NCP and C additives and the absence of oxygen led to increasing the CVs of the developed blends by increasing

Fig. 2. Nanoparticle blend preparation.

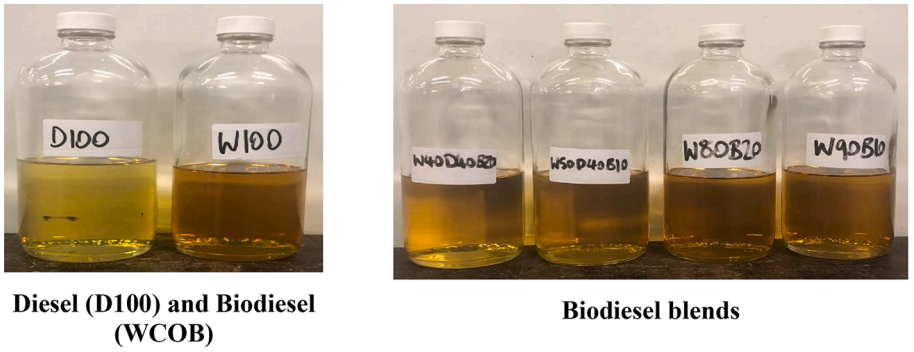

Fig. 3. Pictorial view of the synthesised fuel blends.

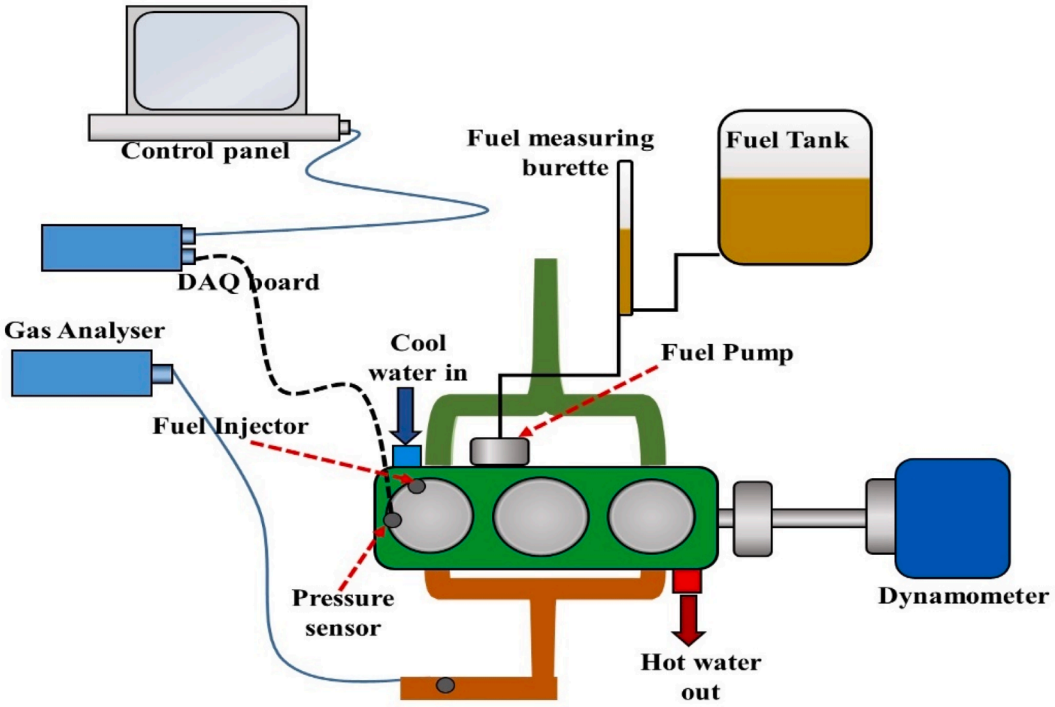

Fig. 4. Schematic of experimental engine test-rig.

Table 3
Engine specifications.

Engine model	LPWS Bio3
Engine manufacture	Lister Petter, UK
Number of cylinders	3
Bore/stroke	86x88 mm
Cylinder volume	1.395 L
Rated speed	1500 rpm
Engine power	9.9 kW
Fuel injection timing	20 deg. bTDC
Compression ratio	22

Table 4
Exhaust gas emission analyser specifications.

Designation	Measuring range	Resolution
CO	o-10% vol.	0.001% vol.
CO_2	0–18% vol.	0.01% vol.
HC	0–9999% ppm vol.	1.0 ppm vol.
O_2	0–22% vol.	0.01% vol.
NO	0–5000 ppm vol.	1.0 ppm vol.
Diesel Smoke meter		
Degree of opacity	0–100%	1%
Absorption coefficient	0–10 m^{-1}	0.01 m^{-1}

their percentage [36]. For example, the CV for B40NCP0.5 was 0.18% lower than B40NCP1, and CV of B40C0.5 was 0.30% lower than B40C1. Furthermore, the CV for C additive blends (B40C1) was approximately 1.5% lower than B40NCP1. The percentage changes in CV for all blends for diesel fuel and neat biodiesel are presented in Fig. 5.

The fuel characterisation revealed the potential of NCP and C additives to enhance the fuel properties. Therefore, the following section will utilise the experimental engine setup to study the combustion characteristics of three selected blends based on their high CV and low viscosity and benchmark them with fossil diesel (D100) and waste cooking oil biodiesel (W100): B40, B40NCP1 and B40C1.

Table 5
Physical properties of fuel blends.

Sl. No.	Blend samples	Density (kg/L)	Calorific value (MJ/kg)	Flash point (°C)	Viscosity (40 °C) mm^2/s
0	D100	0.832	44.1093	63	2.820
0.5	W100	0.88	39.9896	165	5.563
1	B40	0.846	40.0192	72	2.864
2	B40NCP0.5	0.846	41.0146	70	3.225
3	B40NCP1	0.847	41.0896	71	3.262
4	B40C0.5	0.845	40.3169	70	2.869
5	B40C1	0.845	40.4383	70	2.933
6	B50	0.852	39.2457	82.5	3.055
7	B50NCP0.5	0.853	41.107	82	3.247
8	B50NCP1	0.854	41.1423	82	3.440
9	B50C0.5	0.853	39.6309	81.5	3.342
10	B50C1	0.854	40.866	82	3.291
11	B80	0.86	38.7568	77	3.500
12	B80NCP0.5	0.858	39.298	76.5	3.755
13	B80NCP1	0.859	39.822	76.5	3.851
14	B80C0.5	0.858	39.2269	75.5	3.680
15	B80C1	0.859	39.1064	76	3.527
16	B90	0.87	37.8642	89	3.947
17	B90NCP0.5	0.865	38.524	87.5	4.145
18	B90NCP1	0.866	38.66	88	4.214
19	B90C0.5	0.869	38.082	87.5	4.255
20	B90C1	0.87	38.0804	87.5	4.223
21	Butanol [33]	0.794	33.63	35–37	3.64
	EN14214 [34]	0.86–0.90	–	>120 °C	3.5–5

3.2. Engine combustion analysis

Fuel properties of three samples, such as B40, B40NcP1 and B40C1 were found to be close to diesel fuel. Therefore, these blends were selected for engine testing. The combustion characteristics of the selected fuels were studied by determining several factors, such as in-cylinder pressure, heat release rate (HRR), the start of combustion (SoC), end of combustion (EoC), burn duration (BD), ignition delay (ID)

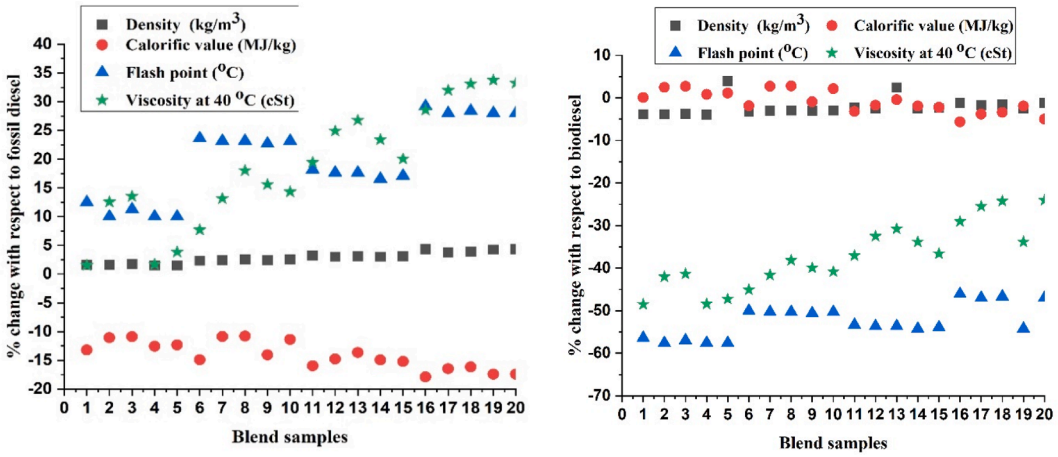

Fig. 5. Fuel characteristics analysis.

at crank angle position (CA), as listed in Table 6. In addition, the rate of the premixed combustion phase can be determined through in-cylinder gas pressure and heat release rate [34].

3.2.1. Start of combustion and combustion duration

Fig. 6 shows the influence of combusting the selected blends at different engine loads on the start of combustion (SoC), end of combustion (EoC), burn duration (BD) and the ignition delay (ID). The start of combustion (SoC) was taken at a crank angle of 5% of the total heat released, and the end of combustion (EoC) was taken at 90% of the total heat released [34]. The start of injection (SoI) was constant at 20 °CA bTDC for all the tested fuels.

D100 showed the earliest start of combustion at all loads compared to other fuel blends, as shown in Fig. 6c. The SoC for W100, B40, B40NcP1 and B40C1 were retarded by 0.28°, 0.35°, 1.51° and 1.21°CA compared to diesel fuel at low engine load (20%). Similarly, compared to W100, SoC for B40NcP1 and B40C1 blends were retarded at about 1.23 CA and 0.83 CA at low engine load (20%). The delay in SoC was due to the higher viscosity and low in-cylinder temperature at low engine load. In addition, the presence of butanol affected the SoC due to its higher latent heat of vaporisation and hence delayed the SoC [36]. It is observed that the SoC was retarded for all the blends compared to W100 even though W100 has a higher viscosity. Neat biodiesel (W100) has a higher cetane number than diesel [37]. The higher the cetane number lower the delay [34]. The cetane number of the B40 blend is lower than B100 due to the addition of butanol in the blend. Due to this reason, B40 gave a higher delay than other fuels. The higher latent heat of vaporisation of butanol slowed the combustion process early by absorbing heat from the compressed air to reach the combustible mixture [38].

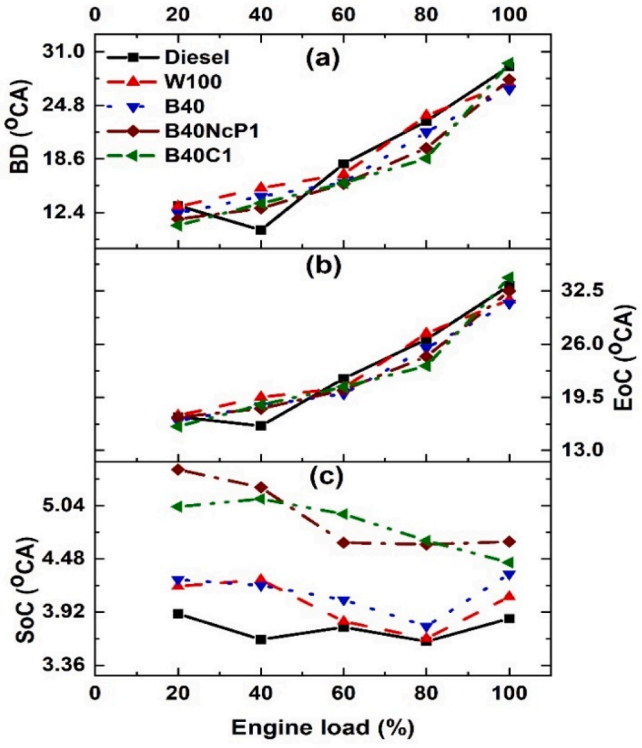

Fig. 6. Combustion charateristics.

Increasing the engine load advanced the SoC for all the blends fuels averagely by 0.23–0.81 % at full load due to the increased in-cylinder temperature [32]. Graphite additive in B40C1 showed a slightly advanced SoC than graphene platelets B40NcP1 due to graphite NP's higher reactivity and lower viscosity in the B40C1 blend that improved the fuel spray and combustion characteristics [32]. At full engine load (100%), SoC for NP additives blends was retarded by about 0.57 °CA and 0.35° CA compared to W100; and 0.81 °CA and 0.58 °CA compared to D100 fuel (Fig. 6c). At high loads, the EoC for W100 fuel was found to be similar to fossil diesel (Fig. 6b). The nanoparticles blends combusted earlier than fossil diesel and W100 fuels (Fig. 6b). Higher thermal conductivity (Table 1) and higher in-cylinder temperature at higher loads led to combust nano-additives blends quicker than other fuels.

The burn duration (BD) is defined as the interval between the SoC and EoC. The BD increases with increasing the engine load due to high fuel injection quantity per stroke [37]. Overall, blends with NcP and C additives showed shorter BD at almost all loads. However, it was observed that at full load, the BD of C additive was almost similar to fossil diesel (Fig. 6a). The delay in SoC and ID can also be confirmed from the fuel injection pressure and maximum in-cylinder pressure in the following sections.

3.2.2. In-cylinder pressure and heat release

Fig. 7 shows the in-cylinder pressure, heat release and fuel injection pressure profiles at various engine loads: low 20%, medium 60% and full load 100%. It can be observed that D100 and fuel blends with NP additives showed higher in-cylinder pressures than W100 and B40 at low engine load, as shown in Fig. 7a. The D100 and fuel blends with NP additives have lower cetane number than W100 and B40 fuels.

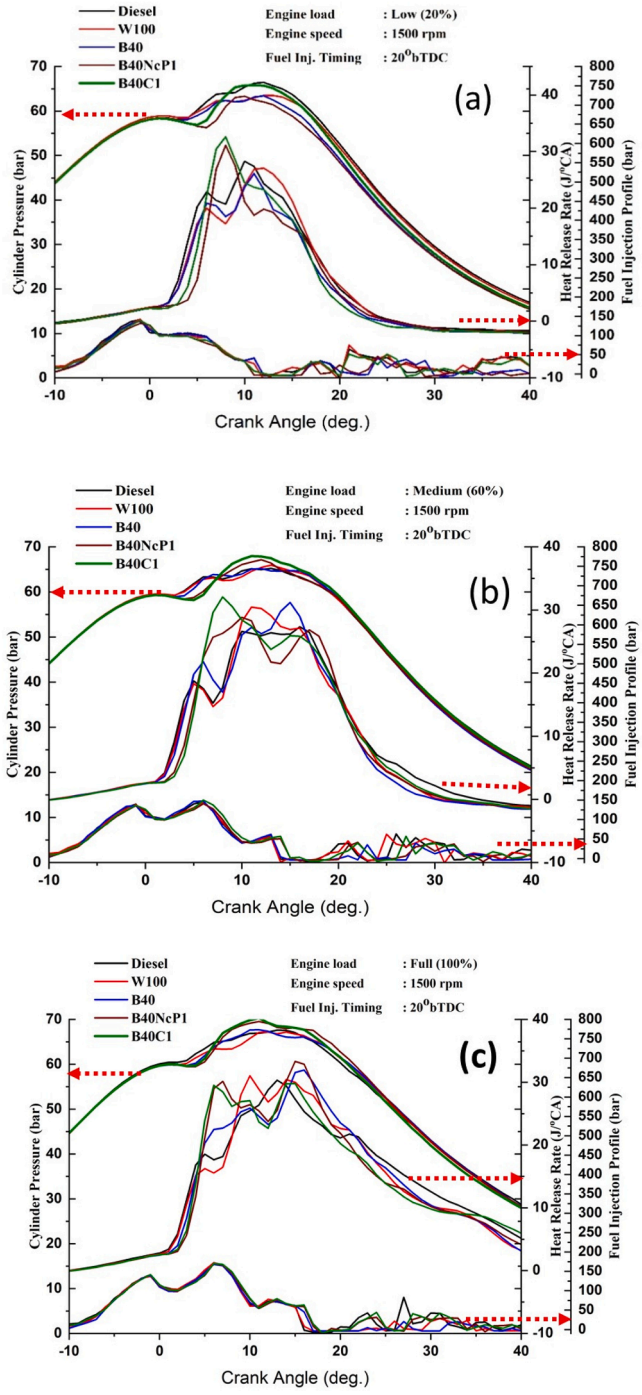

Fig. 7. Variation of the in-cylinder pressure, heat release and fuel injection pressure.

Furthermore, at low loads, the in-cylinder temperature is relatively low. Combined effects of low in-cylinder temperature and higher ignition delay (due to low cetane number) caused more fuel to burn in the premixed combustion phase, which gave higher in-cylinder pressure [37]. Whereas in-cylinder pressure for NP blends increased with increased engine load at medium and full load conditions (Fig. 7b & 7c). While increasing the engine torque increases the fuel injection quantity/strokes, hence increasing the in-cylinder temperature [37]. This phenomenon also increases the fuel injection pressure, as shown in Figs. 7 and 8, at each engine load. The fuel quantity/stroke is less at lower engine load, the pumping force used by the fuel pump is lower, but fuel quantity increases with engine load. Therefore, the fuel pump has to

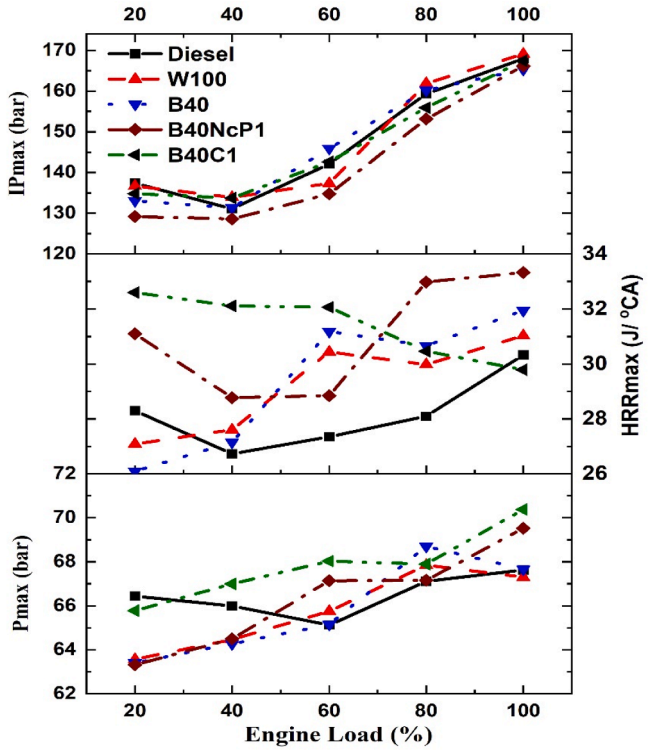

Fig. 8. Maximum cylinder pressure, heat release and fuel injection pressure.

apply more force to inject the required quantity of fuel/stroke [37]. Hence, fuel injection pressure also increased with engine load (Fig. 7 a-c).

The heat release rate (HRR) increases with engine load due to the higher fuel injected per stroke [32]. Therefore, blends with NP additive showed higher HRR at low load and close to diesel at full load, as shown in Figs. 7 and 8. In addition, blends with NP additives showed a high heat release rate compared to D100, W100 and B40 at all engine loads.

Fig. 8 shows the maximum in-cylinder pressure (P_{max}), heat release rate (HRR_{max}) and fuel injection pressure versus engine load. It is observed that maximum in-cylinder pressure (Pmax) increases with engine load (Fig. 8). Pmax for B40NcP1 and B40C1 was observed to be about 63 bar and 65 bar at low load, 67 bar and 68 bar at medium load, and 69 bar and 70 bar at full engine load. It means that B40C1 showed higher in-cylinder pressure at all engine loads. Due to lower viscosity (Table 5) of the B40C1 than B40NcP1, enhanced the fuel spraying and combustion efficiency [27]. Moreover, as shown in Table 1, the lower conductivity and diffusivity of graphite (C) nanoparticles made this material easily combustible during the combustion process. Therefore, Pmax values for B40NcP1 and B40C1 were increased by 0.5–2.5% at full engine load compared to diesel fuel.

The HRR_{max} for B40NcP1 and B40C1 was 9% and 15% higher than D100 and 14% and 16% than W100 at 20% engine load. However, at full load, HRRmax was 9% and 7% higher than D100 and W100 for B40NcP1. Higher HRR results from longer ignition delay (ID), as longer ID allows more fuel to burn in the premixed combustion phase, and due to the sudden explosion, more heat released by the fuel results in higher HRR [39]. Blend with graphite additive (B40C1) showed lower HRR by 1.7% and 4% than D100 and W100 at full load. At full load, the in-cylinder temperature was higher; therefore, the ID period for the B40C1 blend was shorter than B40NcP1, which led to less fuel burn in the premix combustion phase and prolonged the diffusion combustion; hence HRR for B40C1 was reduced at full engine load. In general, NP additive fuels showed higher HRR due to longer ID. Higher viscosity increased the total ID period, which increased the premixed combustion phase. More fuel gets burnt in this phase than in the diffusion

combustion phase. Moreover, nanoparticles' good conductivity and diffusivity (Table 1) made these materials easily combustible during the combustion process. Therefore, it increased the overall combustion efficiency.

3.2.3. The integrated heat release rate

Fig. 9 shows the integrated heat release rate for the investigated fuels at different engine loads. Because of the lower calorific value of the fuel blends, the integrated heat release rate (IHRR) for the fuel blends was lower than fossil diesel for low and medium engine loads but closer to the diesel fuel at maximum engine load. The fuel combustion rate was lowered because the in-cylinder temperature was lower under low load conditions [16,39]. Furthermore, 1-butanol lowered the autoignition temperature because of its higher latent heat of vaporisation, slowing the combustion rate efficiency [39].

3.3. Engine performance characteristics

3.3.1. Brake thermal efficiency

Fig. 10 shows the Brake Thermal Efficiency (BTE) of the investigated fuel blends at different engine loads. The BTE is the fuel conversion efficiency, which equals the braking power to the heat equivalent of the consumed fuel [32]. In general, the BTE for all fuel blends were lower than diesel fuel due to the lower energy contents (CV) [27]. For example, BTE values for B40NcP1 and B40C1 were lower by 11% and 10% at 20% load, but 10% and 8% higher than D100 at full load. At full load, higher in-cylinder temperature and additional oxygen content in butanol helped to improve the fuel combustion efficiency of the blends [40]. Moreover, nanoparticles' higher conductivity and diffusivity (Table 1) made these materials easily combustible during the combustion process. Therefore, it increased the overall combustion efficiency and improved the BTE. Compared to W100, BTE for B40NcP1 and B40C1 were 0.7% and 0.2% lower at 20% engine load due to the lower in-cylinder temperature and higher heat of vaporization of butanol. Furthermore, it was observed that BTE for B40NcP1 and B40C1 increased by increasing engine load. Compared to W100, BTE values for B40NcP1 and B40C1 were higher by 7% and 11% at medium load and 10% and 8% at full engine load. Nanoparticles' higher surface to volume ratio and higher heat transfer rate (due to higher thermal conductivity), along with higher oxygen content (due to butanol) caused higher BTE when the engine was operated with blends [16,30,32]. The faster heat transfer rate in the fuel improved the combustion quality, prompting higher power output [27,41]. Due to lower viscosity and additional oxygen content (from butanol), B40 fuel gave higher BTE than W100 fuel (Fig. 10).

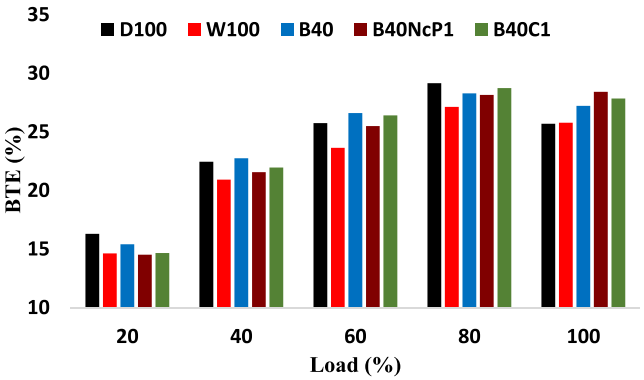

Fig. 10. Variation in BTE with engine load.

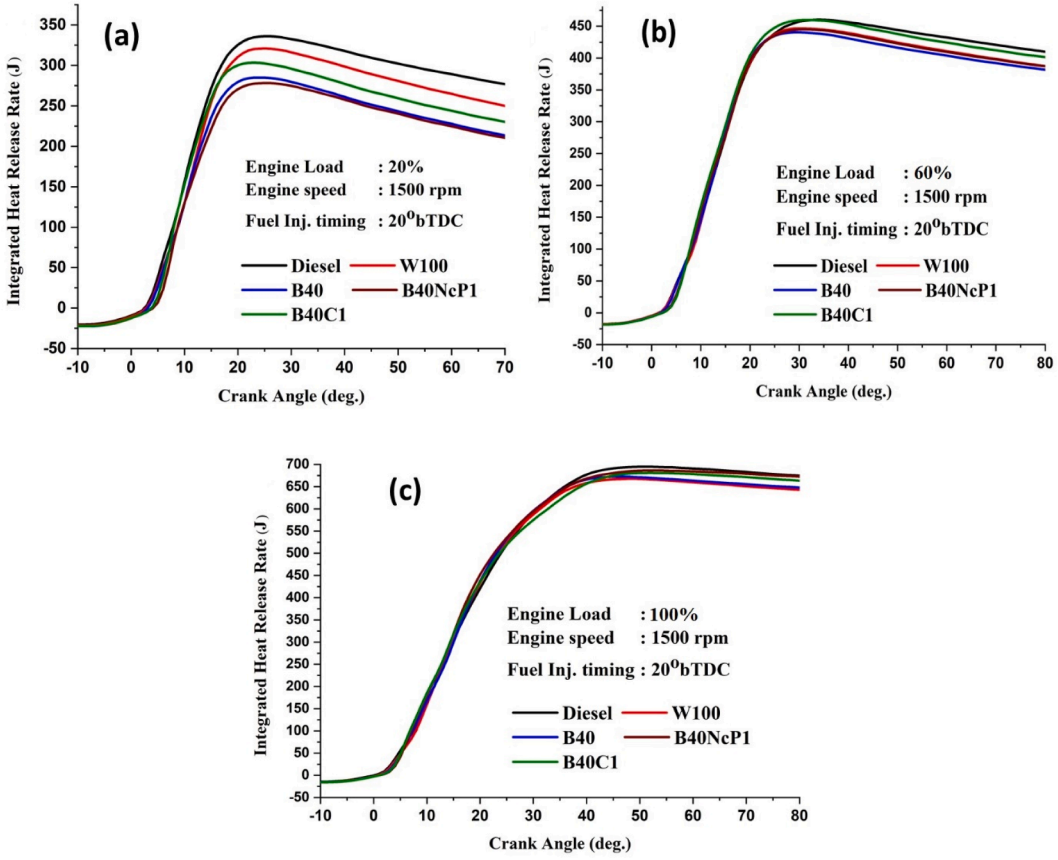

Fig. 9. Variation in integrated heat release with respect to crank angle (CA).

3.3.2. Brake specific fuel consumption

Fig. 11 shows the brake specific fuel consumption (BSFC) for the investigated fuel blends at different engine loads. BSFC measures how well an engine utilises the fuel to meet power demand. When a combustion event or combustion phasing happens near the TDC, the BSFC is reduced [32]. The combustion efficiency of the fuel also affects BSFC, as better combustion efficiency results in lower BSFC. It was observed that BSFC values for W100 and all blends were higher than diesel fuel. It was due to lower heating values and higher viscosity of biodiesel and fuel blends [32]. BSFC for B40NcP1 and B40C1 values were 15% and 16% higher at low engine load and 4% and 2% higher at medium load, but it decreased by 2.8% and 3.2% at full engine load compared to diesel fuel. While compared to W100, BSFC values were 1.9% and 1.2% lower for B40NcP1 and B40C1 at low load, 9.7% and 11% lower at medium load and 8% and 8.4% lower at full engine load. At this point, it can be concluded that blends with NP additive have BSFC lower than W100 due to lower viscosity, higher CV, and better combustion efficiency due to nanoparticle addition [41].

3.4. Emission analysis

3.4.1. Nitrogen oxide

Fig. 12 depicts the nitric oxide (NO) change with load for the investigated fuel blends benchmarked against Diesel (D100). The NO emission for diesel was higher than for biodiesel and its blends; therefore, biodiesel's emission characteristics were better than present neat diesel [32]. It was observed that NO emissions increased for all fuels by increasing the engine load. Increasing the engine load increased the in-cylinder temperature, which improved the fuel/air mixing rate. This resulted in better fuel combustion efficiency and increased the formation of thermal NO emissions [32]. NO emissions were reduced with the addition of the nanoparticles compared to the D100 and W100 at medium and full engine load. The NO is mainly formed during the premixed combustion due to high combustion temperature. When we added the NP as an additive in fuel, they were observed some heat from the combustion to oxidise. This harmed cylinder temperature.

Therefore, NO was reduced slightly in the case of NP additive. NO emissions for B40NcP1 and B40C1 were found 1.5% and 2.3% lower at 20% load, 10.8% and 10.05% lower at 60% medium load and 5% and 0.3% lower at full engine load than D100, respectively. Whereas NO emissions for B40NcP1 and B40C1 were 1.7% and 1% higher at 20% load, 1.4% and 2.5% lower at 60% load compared to W100. But it reduced at full engine load by 5% and 0.7%, respectively. Blends with graphite additives (B40C1) showed overall higher NO emissions than blends with graphene additives (B40NcP1) because of better combustion due to lower conductivity and diffusivity (Table 1). Low viscous fuel improved the fuel spray and vaporisation characteristics, improving fuel combustion faster. The increase in the in-cylinder temperature results in higher NO emissions [32].

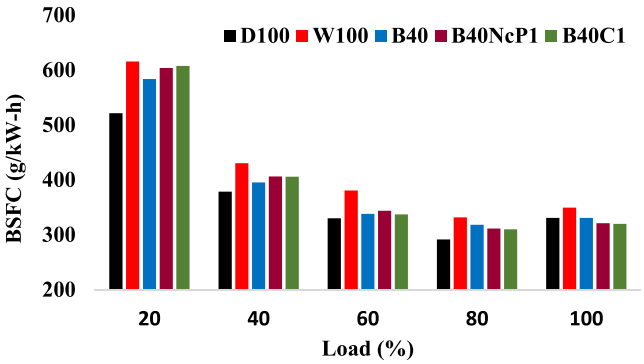

Fig. 11. Variation in BSFC with engine load.

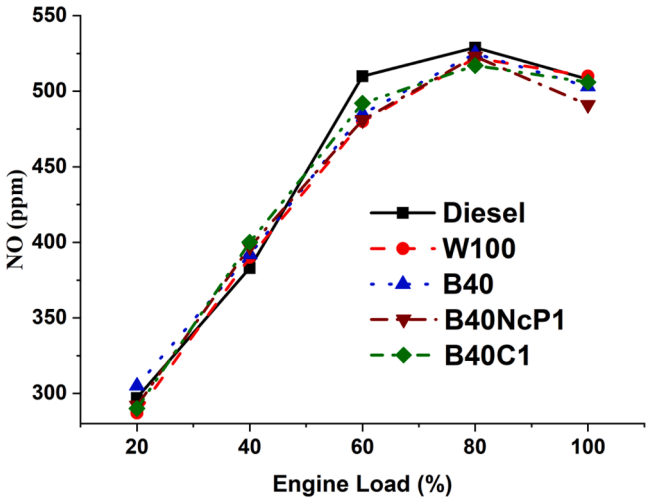

Fig. 12. NO emission versus engine load.

3.4.2. Carbon monoxide and carbon dioxide and engine load

Fig. 13 shows varying the engine load on the carbon emissions (i.e., CO and CO_2) for the investigated fuels. Carbon monoxide (CO) emissions results from incomplete combustion due to the non-homogeneous fuel–air mixing in the engine. It occurs due to the lack of oxygen within the cylinder (fuel-rich zone) or at low local combustion

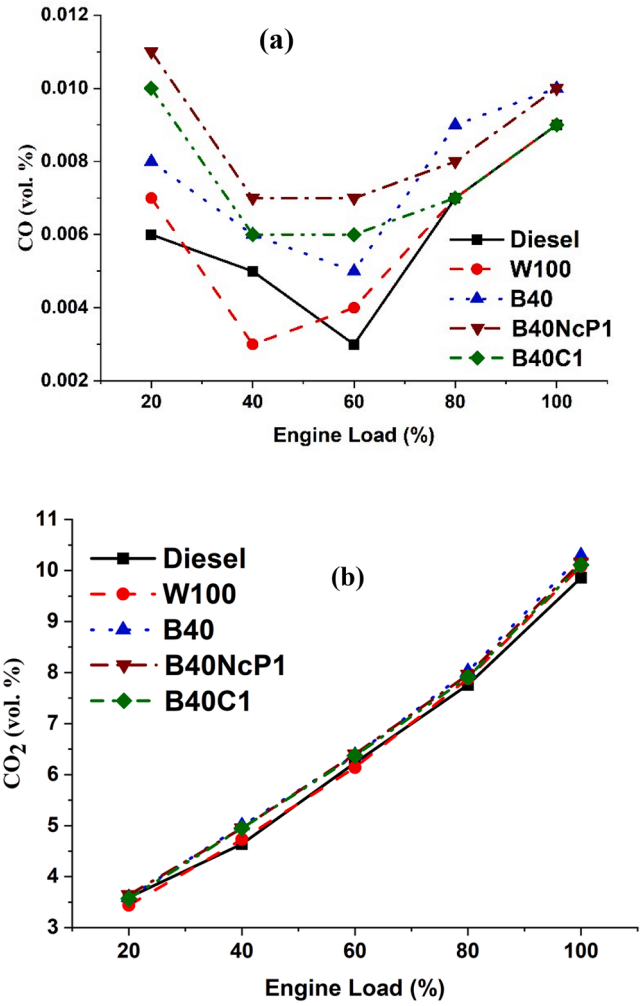

Fig. 13. Variation in (a) CO and (b) CO_2 formation versus engine load.

temperature [32]. CO values for the blended fuel were higher at low-to-medium engine loads (Fig. 13a) due to the addition of butanol. Higher latent heat of butanol reduced the in-cylinder temperature, which slowed down the oxidation rate of CO to CO2. The CO emissions for B40NCP1 and B40c1 were higher by 83% and 66% at low load (20%) 57% and 50% at medium load (60%), and 11% and 0.1% at full engine load as compared to D100 (Fig. 13a). CO emissions for B40NCP1 and B40C1 were higher by 57% and 42% at low load (20%), 75% and 50% at medium load (60%) and 11% and 0.1% at full engine load than W100, respectively. It is observed that blends with NP additive emitted more CO because the NP additive absorbed in-cylinder combustion heat to reach the combustible limit; this may again reduce the oxidation rate of CO [32].

Furthermore, due to the latent heat of vaporisation, the addition of butanol slowed the oxidation of CO to CO_2. As a result, it was found that CO emission is higher for blend fuels than diesel and W100. Therefore, the formation of CO_2 was observed to be at the optimum level with blends (Fig. 13b). Besides, B40C1 showed an overall lower CO_2 emission than B40NcP1 (Fig. 13b) due to lower conductivity and diffusivity of NP doses (Table 1).

3.4.3. Smoke and engine load

Fig. 14 shows the capacity versus engine load for the investigated fuels. The smoke emission formation is primarily due to incomplete combustion and is influenced by the fuel's viscosity, spray characteristics, and in-cylinder temperature [32,39]. In this study, smoke emissions increased with increasing engine load. W100 showed higher smoke opacity than D100 and blends with NP additives due to their higher viscosity which affects spray characteristics and causes incomplete combustion; this agrees with a previous study by Sharma et al.[34]. Smoke emissions for B40NCP1 and B40C1 were similar to D100 and B40 at all engine loads. Besides, adding butanol to the blends lowered the temperature by absorbing its high heat of vaporisation, resulting in incomplete combustion, as previously observed by Thakkar et al. [36]. The high in-cylinder temperature reduced such an impact under full load.

4. Conclusion and prospects

This article aimed to study the broader application of few-layered graphene and graphite as fuel additives to enhance the engine's emissions combustion characteristics. Therefore, graphene and graphite nanoparticles' various dosages in waste cooking biodiesel blends and their impact on combustion and engine performance were investigated. Initially, 22 fuels, including fossil diesel and waste cooking oil biofuel, were synthesised and characterised. Then, experiments were conducted on the engine with five fuels under variable loads at a constant speed of 1500 rpm: fossil Diesel D100, W100, B40, B40NCP1and B40C1. An emphasis was on utilising waste cooking oil biodiesel to promote its uptake, hence fostering the circular bioeconomy and disposing of it safely. The key findings can be concluded as below.

- Blend with graphite additive (B40C1) showed lower HRR by 1.7% and 4% than D100 and W100 fuels, respectively, at full load.
- Blends with NP additives showed relatively higher viscosity, which extended the start of combustion (SoC), end of combustion (EoC), ignition delay (ID), and the burn duration (BD) for both B40NCP1 and B40C1 fuels.
- Fuel blends with NP additives showed higher BTE at full engine load. B40NCP1 and B40C1 showed an increment in BTE by 8–10% at full engine load compared to D100 and W100 fuels.
- BSFC for biodiesel and fuel blends were higher than fossil diesel. However, B40NCP1 and B40C1 blends gave 8–8.5% lower BSFC than W100 due to their higher heating values.
- Using few-layered graphene and graphite NP in the blend decreased NO gas emissions by 5%, but increased CO_2, CO and smoke emissions compared to fossil diesel. The CO emissions for B40NCP1 and B40C1 were higher by 57% and 42% at low load, 75% and 50% at medium load, and 11% and 0.1% at full load than the W100 fuel, respectively.

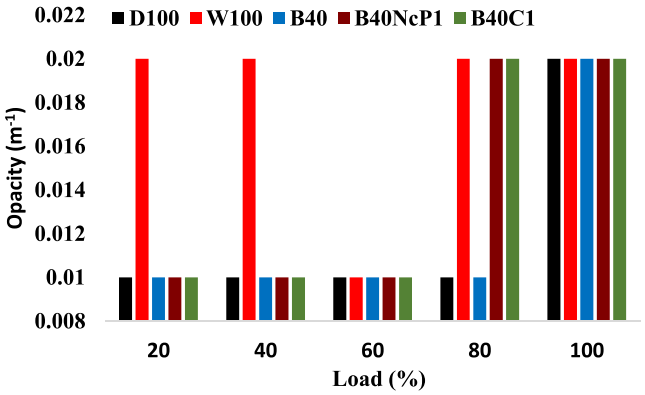

Fig. 14. Smoke formation versus engine load.

Overall, nanoparticle additives in biofuel showed a great potential to control NO emissions and improve engine efficiency. Furthermore, the combustion characteristics suggest that the engine combusts the nanoparticle fuel blends more efficiently; thus, a decrease in NO emissions was distinctive.

Investigating such promising multi-component fuel blends under various engine operating conditions, such as in dual fuel mode under advanced low-temperature combustion, is a topic for further research.

Declaration of Competing Interest

The authors declare that they have no known competing financial interests or personal relationships that could have appeared to influence the work reported in this paper.

Acknowledgements

The authors would like to acknowledge the UKIERI project for funding this work (Grant Number: DST-UKIERI 18-19-04): Waste to Energy - Low-Temperature Combustion of Sustainable Green Fuels.

References

[1] Strzalka R, Schneider D, Eicker U. Current status of bioenergy technologies in Germany. Renew Sustain Energy Rev 2017;72:801–20. https://doi.org/10.1016/j.rser.2017.01.091.
[2] Park SR, Pandey AK, Tyagi VV, Tyagi SK. Energy and exergy analysis of typical renewable energy systems. Renew Sustain Energy Rev 2014;30:105–23. https://doi.org/10.1016/J.RSER.2013.09.011.
[3] Kumar MS, Jaikumar M. A comprehensive study on performance, emission and combustion behavior of a compression ignition engine fuelled with WCO (waste cooking oil) emulsion as fuel. J Energy Inst 2014;87:263–71. https://doi.org/10.1016/J.JOEI.2014.03.001.
[4] Najafi B, Ardabili SF, Mosavi A, Shamshirband S, Rabczuk T. An intelligent artificial neural network-response surface methodology method for accessing the optimum biodiesel and diesel fuel blending conditions in a diesel engine from the viewpoint of exergy and energy analysis. Energies 2018;11. https://doi.org/10.3390/en11040860.
[5] Sanli H. An experimental investigation on the usage of waste frying oil-diesel fuel blends with low viscosity in a Common Rail DI-diesel engine. Fuel 2018;222:434–43. https://doi.org/10.1016/J.FUEL.2018.02.194.
[6] Jain NL, Soni SL, Poonia MP, Sharma D, Srivastava AK, Jain H. Performance and emission characteristics of preheated and blended thumba vegetable oil in a compression ignition engine. Appl Therm Eng 2017;113:970–9. https://doi.org/10.1016/J.APPLTHERMALENG.2016.10.186.
[7] Özer S, Akçay M, Vural E. Effect of toluene addition to waste cooking oil on combustion characteristics of a ci engine. Fuel 2021;303:121284. https://doi.org/10.1016/J.FUEL.2021.121284.
[8] Attia AMA, Hassaneen AE. Influence of diesel fuel blended with biodiesel produced from waste cooking oil on diesel engine performance. Fuel 2016;167:316–28. https://doi.org/10.1016/J.FUEL.2015.11.064.

[9] Hossain AK, Davies PA. Plant oils as fuels for compression ignition engines: A technical review and life-cycle analysis. Renew Energy 2010;35:1–13. https://doi.org/10.1016/J.RENENE.2009.05.009.

[10] Khan HM, Iqbal T, Yasin S, Irfan M, Kazmi M, Fayaz H, et al. Production and utilization aspects of waste cooking oil based biodiesel in Pakistan. Alexandria Eng J 2021;60:5831–49. https://doi.org/10.1016/J.AEJ.2021.04.043.

[11] Ozsezen AN, Canakci M, Turkcan A, Sayin C. Performance and combustion characteristics of a DI diesel engine fueled with waste palm oil and canola oil methyl esters. Fuel 2009;88:629–36. https://doi.org/10.1016/J.FUEL.2008.09.023.

[12] Mohd Noor CW, Noor MM, Mamat R. Biodiesel as alternative fuel for marine diesel engine applications: A review. Renew Sustain Energy Rev 2018;94:127–42. https://doi.org/10.1016/J.RSER.2018.05.031.

[13] Tamilselvan P, Nallusamy N, Rajkumar S. A comprehensive review on performance, combustion and emission characteristics of biodiesel fuelled diesel engines. Renew Sustain Energy Rev 2017;79:1134–59. https://doi.org/10.1016/J.RSER.2017.05.176.

[14] Haghighat Shoar F, Najafi B, Mosavi A. Effects of triethylene glycol mono methyl ether (TGME) as a novel oxygenated additive on emission and performance of a dual-fuel diesel engine fueled with natural gas-diesel/biodiesel. Energy Rep 2021;7:1172–89. https://doi.org/10.1016/J.EGYR.2021.01.088.

[15] Khond VW, Kriplani VM. Effect of nanofluid additives on performances and emissions of emulsified diesel and biodiesel fueled stationary CI engine: A comprehensive review. Renew Sustain Energy Rev 2016;59:1338–48. https://doi.org/10.1016/J.RSER.2016.01.051.

[16] Bidir MG, Millerjothi NK, Adaramola MS, Hagos FY. The role of nanoparticles on biofuel production and as an additive in ternary blend fuelled diesel engine: A review. Energy Rep 2021;7:3614–27. https://doi.org/10.1016/J.EGYR.2021.05.084.

[17] Inês IA, Silva ARR, Moita ASOH, Mendes MAA, Costa MMG. Combustion characteristics of a single droplet of hydroprocessed vegetable oil blended with aluminum nanoparticles in a drop tube furnace. Fuel 2021;302:121160. https://doi.org/10.1016/J.FUEL.2021.121160.

[18] Ağbulut Ü, Polat F, Sarıdemir S. A comprehensive study on the influences of different types of nano-sized particles usage in diesel-bioethanol blends on combustion, performance, and environmental aspects. Energy 2021;229:120548. https://doi.org/10.1016/J.ENERGY.2021.120548.

[19] Purushothaman P, Masimalai S, Subramani V. Effective utilization of mahua oil blended with optimum amount of Al2O3 and TiO2 nanoparticles for better performance in CI engine. Environ Sci Pollut Res 2021;28:11893–903. https://doi.org/10.1007/s11356-020-07926-x.

[20] Jaikumar S, Srinivas V, Rajasekhar M. Influence of dispersant added nanoparticle additives with diesel-biodiesel blend on direct injection compression ignition engine: Combustion, engine performance, and exhaust emissions approach. Energy 2021;224:120197. https://doi.org/10.1016/J.ENERGY.2021.120197.

[21] Jabraeili M, Pourdarbani R, Najafi B, Nematollahzadeh A. Modelling the Effects of Al 2 O 3 -SiO_2 Nanocomposite Additive in Biodiesel – Diesel Fuel on Diesel Engine Performance using Hybrid ANN-ABC 2021:20–6. https://doi.org/10.2478/ata-2021-0004.

[22] Lobo A, Ramesh DK, Chowdhury DR. The effect of Zinc Oxide on Operation of Compression Ignition Engine with EGR fueled with Waste Cooking Oil Biodiesel 2021;1013:1–13. https://doi.org/10.1088/1757-899X/1013/1/012037.

[23] Gadipelli S, Guo ZX. Graphene-based materials: Synthesis and gas sorption, storage and separation. Prog Mater Sci 2015;69:1–60. https://doi.org/10.1016/J.PMATSCI.2014.10.004.

[24] Mahanta NK, Abramson AR. Thermal conductivity of graphene and graphene oxide nanoplatelets. Intersoc Conf Therm Thermomechanical Phenom Electron Syst ITHERM 2012:1–6. https://doi.org/10.1109/ITHERM.2012.6231405.

[25] Hoseini SS, Najafi G, Ghobadian B, Mamat R, Ebadi MT, Yusaf T. Novel environmentally friendly fuel: The effects of nanographene oxide additives on the performance and emission characteristics of diesel engines fuelled with Ailanthus altissima biodiesel. Renew Energy 2018;125:283–94. https://doi.org/10.1016/J.RENENE.2018.02.104.

[26] Nagaraja S, Dsilva Winfred Rufuss D, Hossain AK. Microscopic characteristics of biodiesel – Graphene oxide nanoparticle blends and their Utilisation in a compression ignition engine. Renew. Energy 2020;160:830–41. https://doi.org/10.1016/J.RENENE.2020.07.032.

[27] Hoseini SS, Najafi G, Ghobadian B, Ebadi MT, Mamat R, Yusaf T. Biodiesels from three feedstock: The effect of graphene oxide (GO) nanoparticles diesel engine parameters fuelled with biodiesel. Renew Energy 2020;145:190–201. https://doi.org/10.1016/J.RENENE.2019.06.020.

[28] Hoseini SS, Najafi G, Ghobadian B, Ebadi MT, Mamat R, Yusaf T. Performance and emission characteristics of a CI engine using graphene oxide (GO) nano-particles additives in biodiesel-diesel blends. Renew Energy 2020;145:458–65. https://doi.org/10.1016/J.RENENE.2019.06.006.

[29] Ettefaghi E, Rashidi A, Ghobadian B, Najafi G, Ghasemy E, Khoshtaghaza MH, et al. Bio-nano emulsion fuel based on graphene quantum dot nanoparticles for reducing energy consumption and pollutants emission. Energy 2021;218:119551. https://doi.org/10.1016/J.ENERGY.2020.119551.

[30] Chacko N, Jeyaseelan T. Comparative evaluation of graphene oxide and graphene nanoplatelets as fuel additives on the combustion and emission characteristics of a diesel engine fuelled with diesel and biodiesel blend. Fuel Process Technol 2020;204:106406. https://doi.org/10.1016/J.FUPROC.2020.106406.

[31] Hossain AK. Combustion Characteristics of Waste Cooking Oil–Butanol/Diesel/Gasoline Blends for Cleaner Emission. Clean Technol 2020;2:447–61. https://doi.org/10.3390/cleantechnol2040028.

[32] Lv J, Wang S, Meng B. The effects of nano-additives added to diesel-biodiesel fuel blends on combustion and emission characteristics of diesel engine. A Review Energies 2022;15. https://doi.org/10.3390/en15031032.

[33] Kilic G, Sungur B, Topaloglu B, Ozcan H. Experimental analysis on the performance and emissions of diesel/butanol/biodiesel blended fuels in a flame tube boiler. Appl Therm Eng 2018;130:195–202. https://doi.org/10.1016/j.applthermaleng.2017.11.006.

[34] Sharma V, Duraisamy G, Arumugum K. Impact of bio-mix fuel on performance, emission and combustion characteristics in a single cylinder DICI VCR engine. Renew Energy 2020;146:111–24. https://doi.org/10.1016/J.RENENE.2019.06.142.

[35] Sharma V, Duraisamy G. Production and characterization of bio-mix fuel produced from a ternary and quaternary mixture of raw oil feedstock. J Clean Prod 2019;221:271–85. https://doi.org/10.1016/j.jclepro.2019.02.214.

[36] Thakkar K, Kachhwaha SS, Kodgire P, Srinivasan S. Combustion investigation of ternary blend mixture of biodiesel/n-butanol/diesel: CI engine performance and emission control. Renew Sustain Energy Rev 2021;137:110468. https://doi.org/10.1016/j.rser.2020.110468.

[37] Sharma V, Hossain AK. Experimental Investigation of Neat Biodiesels ' Saturation Level on Combustion and Emission Characteristics in a CI Engine Energies 2021;14:5203. https://doi.org/10.3390/en14165203.

[38] Hernández JJ, Lapuerta M, Cova-Bonillo A. Autoignition reactivity of blends of diesel and biodiesel fuels with butanol isomers. J Energy Inst 2019;92:1223–31. https://doi.org/10.1016/j.joei.2018.05.008.

[39] Ooi JB, Ismail HM, Tan BT, Wang X. Effects of graphite oxide and single-walled carbon nanotubes as diesel additives on the performance, combustion, and emission characteristics of a light-duty diesel engine. Energy 2018;161:70–80. https://doi.org/10.1016/j.energy.2018.07.062.

[40] Patil V, Thirumalini S. Effect of cooled EGR on performance and emission characteristics of diesel engine with diesel and diesel-karanja blend. Mater Today Proc 2021;46:4720–7. https://doi.org/10.1016/J.MATPR.2020.10.303.

[41] Shaafi T, Sairam K, Gopinath A, Kumaresan G, Velraj R. Effect of dispersion of various nanoadditives on the performance and emission characteristics of a CI engine fuelled with diesel, biodiesel and blends—A review. Renew Sustain Energy Rev 2015;49:563–73. https://doi.org/10.1016/j.rser.2015.04.086.